

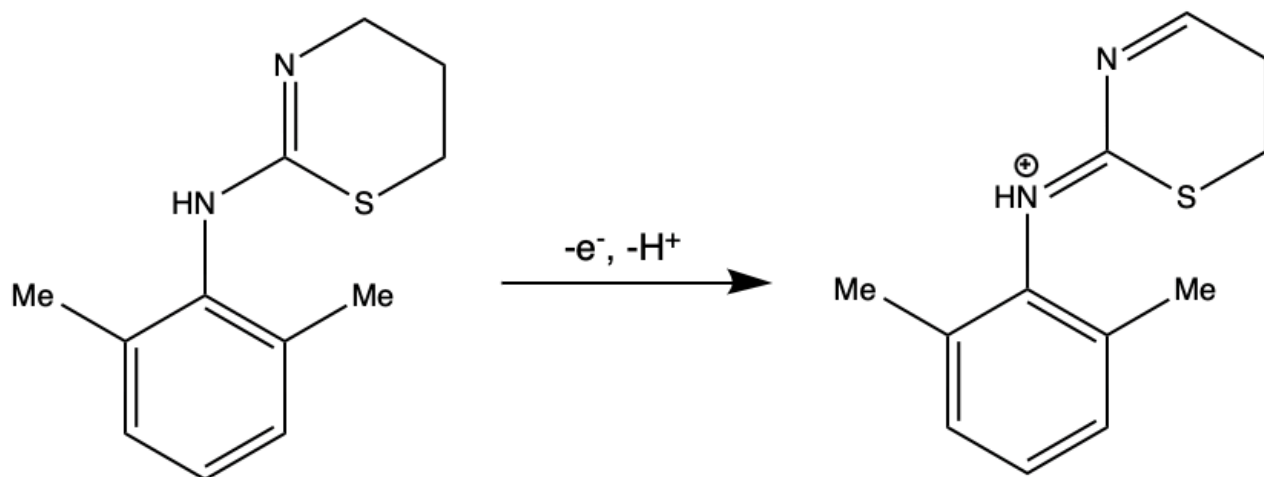
# ***Supplemental Data: Fouling-Resistant Voltammetric Xylazine Sensors for Detection of the Street Drug “Tranq”***

Joyce E. Stern, Ann H. Wemple, Arielle Vinnikov, Charlie W. Sheppard, and Michael C. Leopold\*

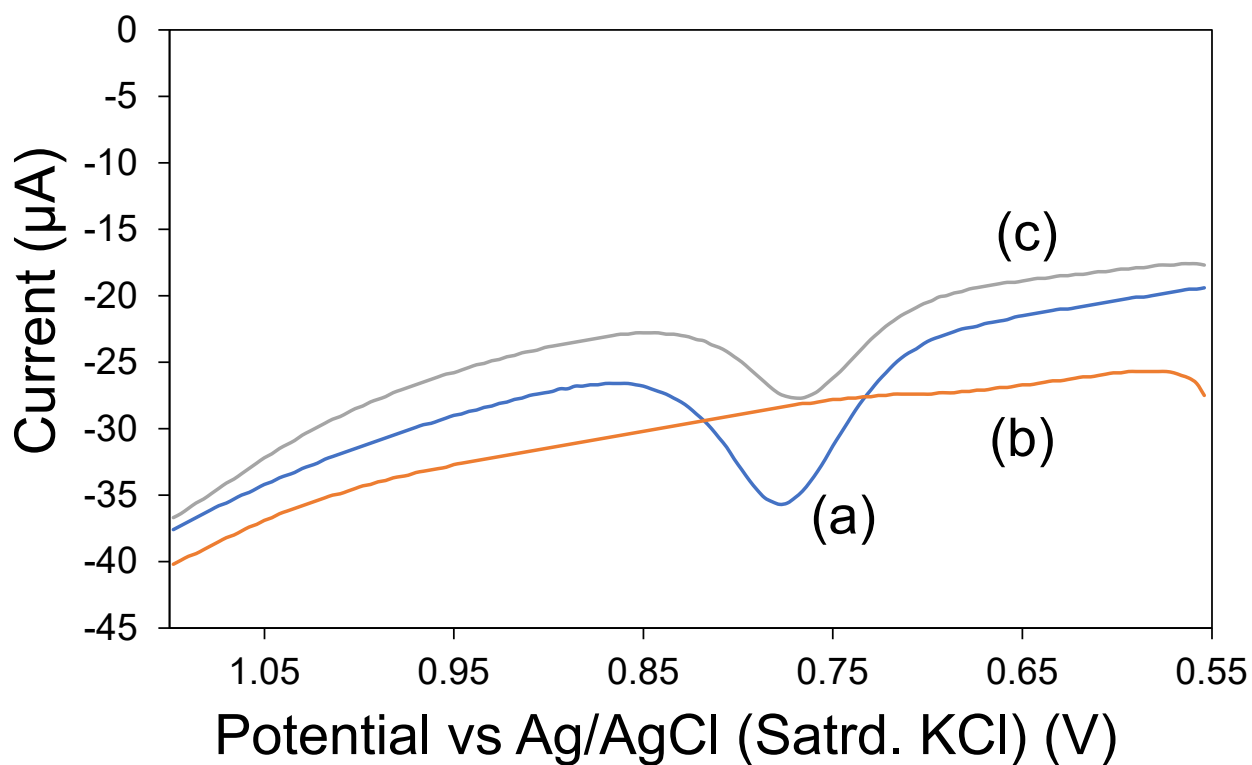
*\*Department of Chemistry, Gottwald Center for the Sciences, University of Richmond, Richmond, Virginia 23173, United States (Corresponding Author)*

## **Table of Contents for Supplemental Data:**

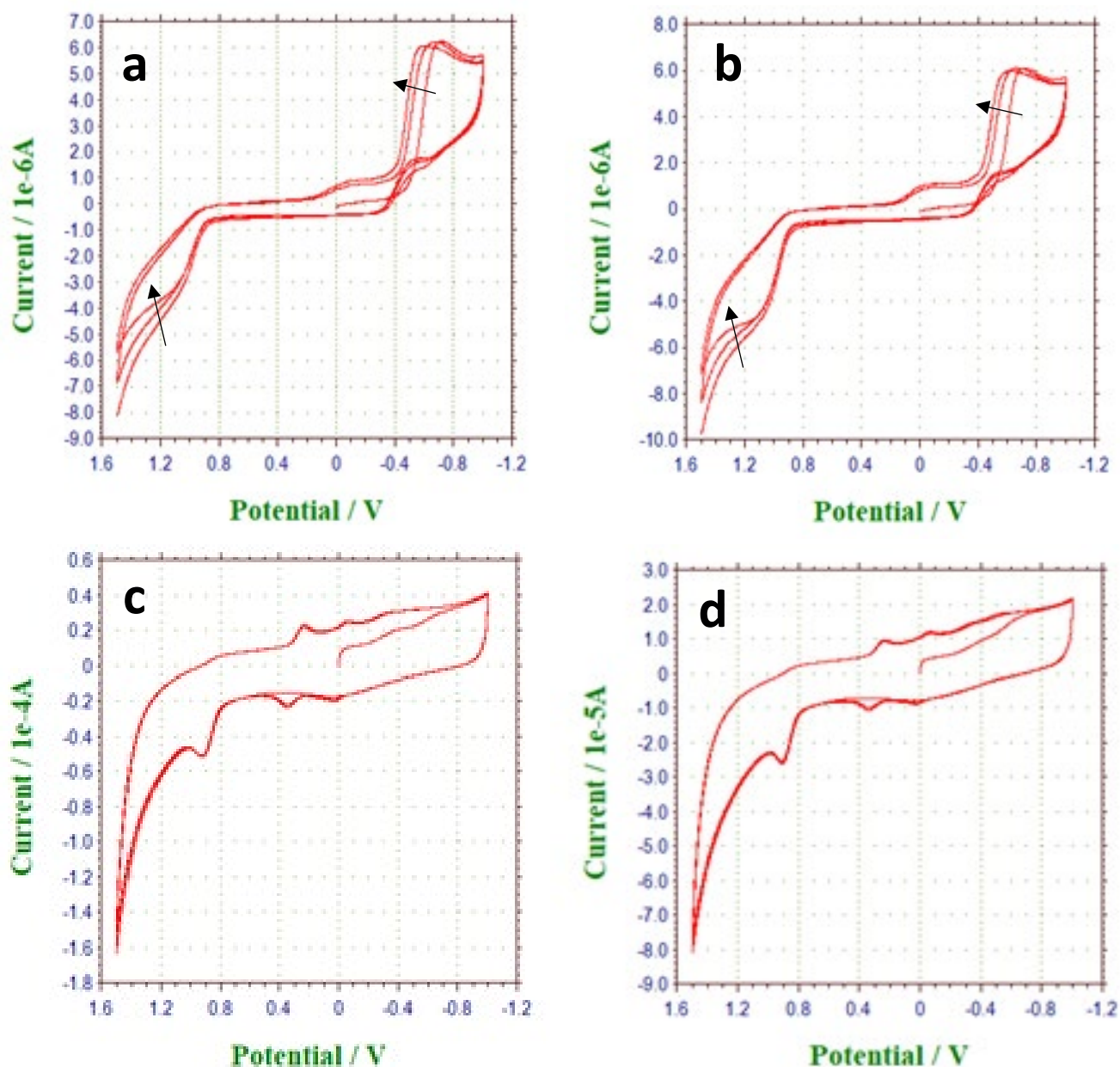
- **Scheme S1:** One proposed mechanism of XYL oxidation
- DPV oxidative scans of XYL, DEHP, and a mixture showing competition for  $\beta$ -CD cavities (selectivity) (**Figure S1**).
- CV analysis of each layer/components effect on voltammetry signal including layer-by-layer (**Figure S2**) and voltammogram overlays (**Figure S3**).
- DPV oxidative scans of 0, 1, and 5 mM XYL solutions showing the concentration dependence and independence of oxidation peaks at  $\sim +0.9$  and  $\sim 0.0$  V, respectively (**Figure S4**).
- Small potential window scan rate analysis of voltametric peaks including XYL oxidation and reduction of its product (**Figures S5-A/B** and **Table S1**).
- Repeated DPV oxidative scans of bare and modified GCE in 255  $\mu$ M XYL showing peak current, peak potential, and fouling effects to XYL exposure (**Figure S6**).
- DPV oxidative scans of a modified GCE in increasing standard XYL concentrations for generating a calibration curve (**Figure S7**).
- DPV oxidative scans of a bare GCE in increasing standard XYL concentrations for generating a calibration curve (**Figure S8**).
- DPV scans of tandem result using both a bare and modified electrode system in different mixtures of XYL, cocaine, and fentanyl (**Figures S9-S10**).
- DPV oxidative scans of XYL and potential interferent species found in solutions of cola and diet cola (**Figure S11**).
- DPV oxidative scans of XYL and potential interferent species found in solutions of vodka and tequila (**Figure S12**).
- DPV generated calibration curves for beverage solutions including simulated soda and diet soda (**Figure S13**), real samples of cola and diet cola (**Figure S14**), diluted cola samples (**Figure S15**), as well as tequila and vodka solutions (**Figure S16**).



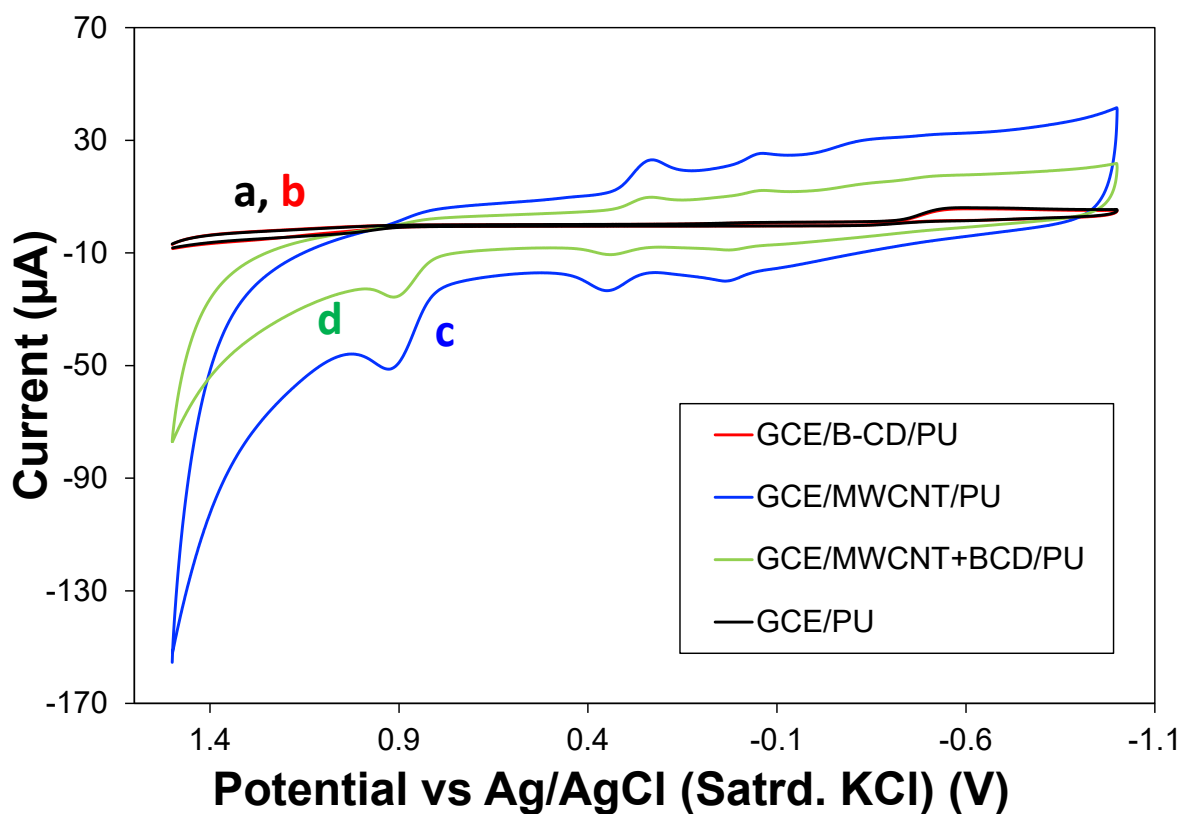
**Scheme S1.** One of the more commonly proposed mechanisms for the oxidation of XYL at an electrode (References). Note: As mentioned in the text, there is no consensus on the exact electrochemical mechanism and/or redox chemistry of XYL, with some reports indicating different multi-step processes, for example.



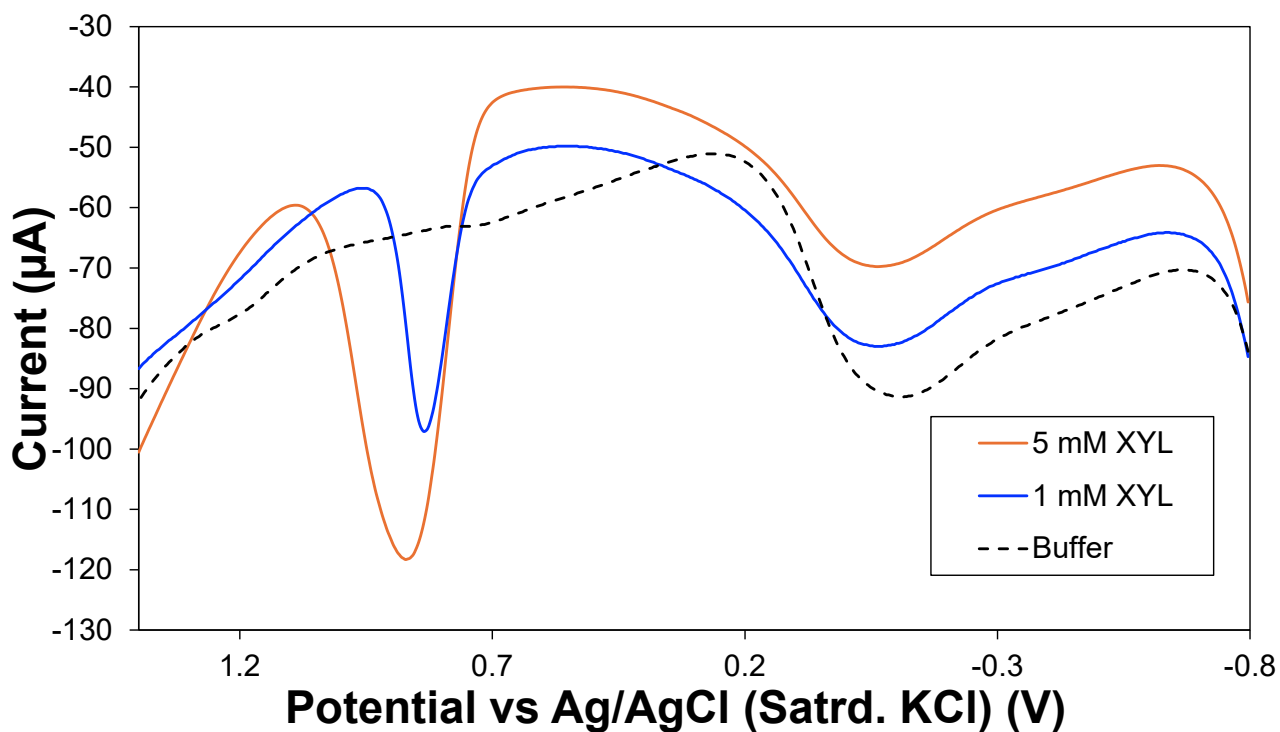
**Figure S1.** DPV oxidative scans of modified GCEs in a solution of (a) 125  $\mu\text{M}$  XYL, (b) 250  $\mu\text{M}$  Di(2-Ethylhexyl)Phthalate (DEHP), and (c) a mixture of 125  $\mu\text{M}$  XYL and 250  $\mu\text{M}$  DEHP showing that peak area is diminished as the DEHP blocks the  $\beta$ -CD binding sites stronger than XYL. Note: All solutions are in 150 mM PBS (pH = 7).



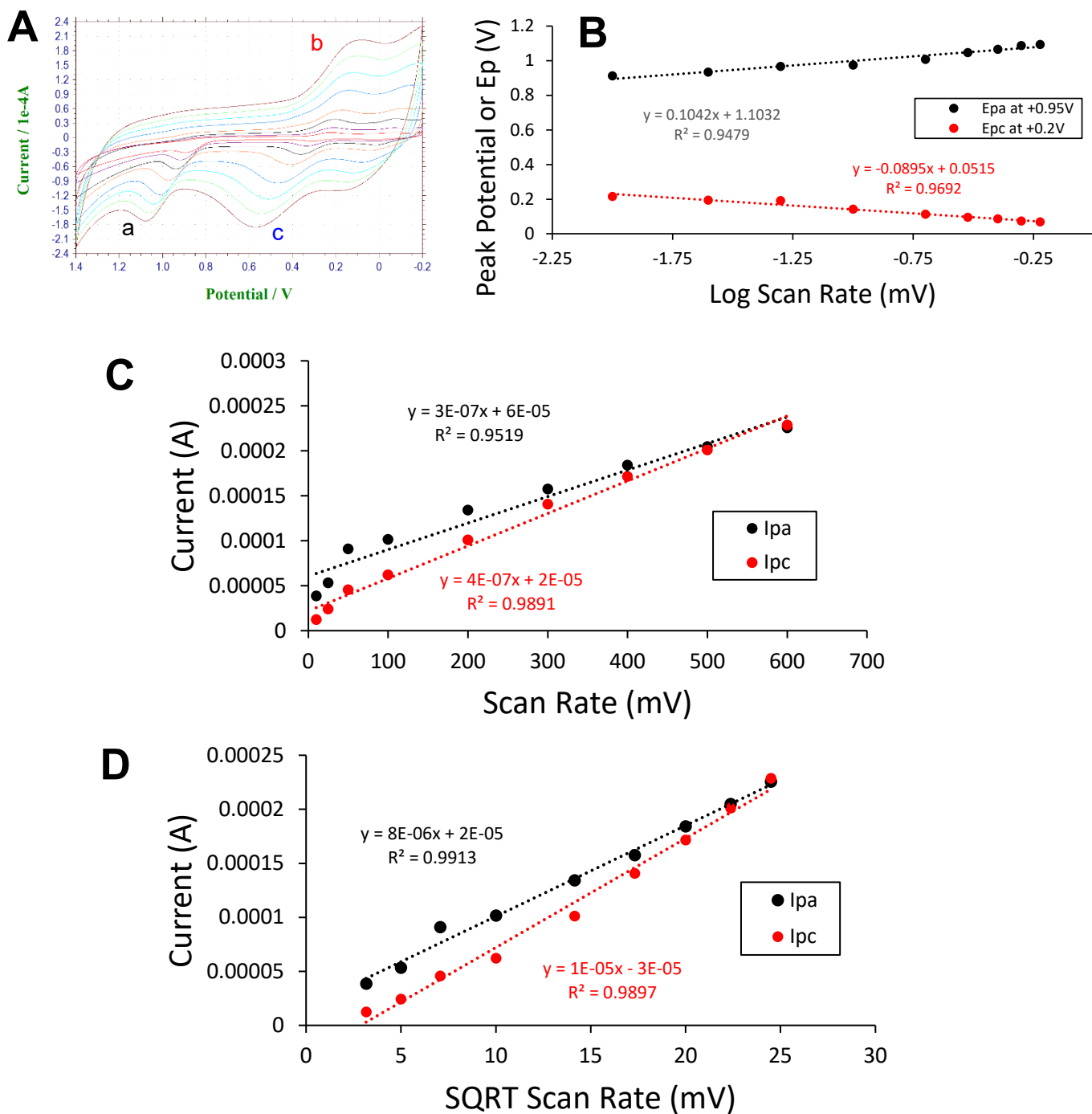
**Figure S2.** Cyclic voltammetry (3 cycles; 6 segments) of various systems (modified electrodes) in 1 mM XYL (150 mM PBS) including **(a)** GCE/PU; **(b)** GCE/ $\beta$ -CD/PU; **(c)** GCE/COOH-MWCNT/PU and; **(d)** GCE/COOH-MWCNT +  $\beta$ -CD/PU (full, optimized modified electrode system). Notes: In the presence of MWCNTs, XYL oxidation potential shifts to more negative potentials (scan rate is 50 mV/sec).



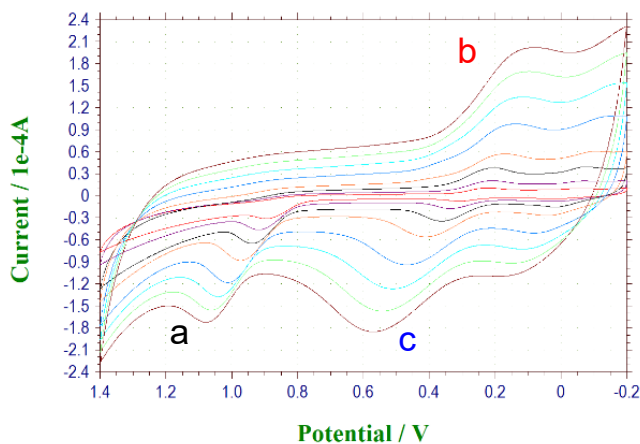
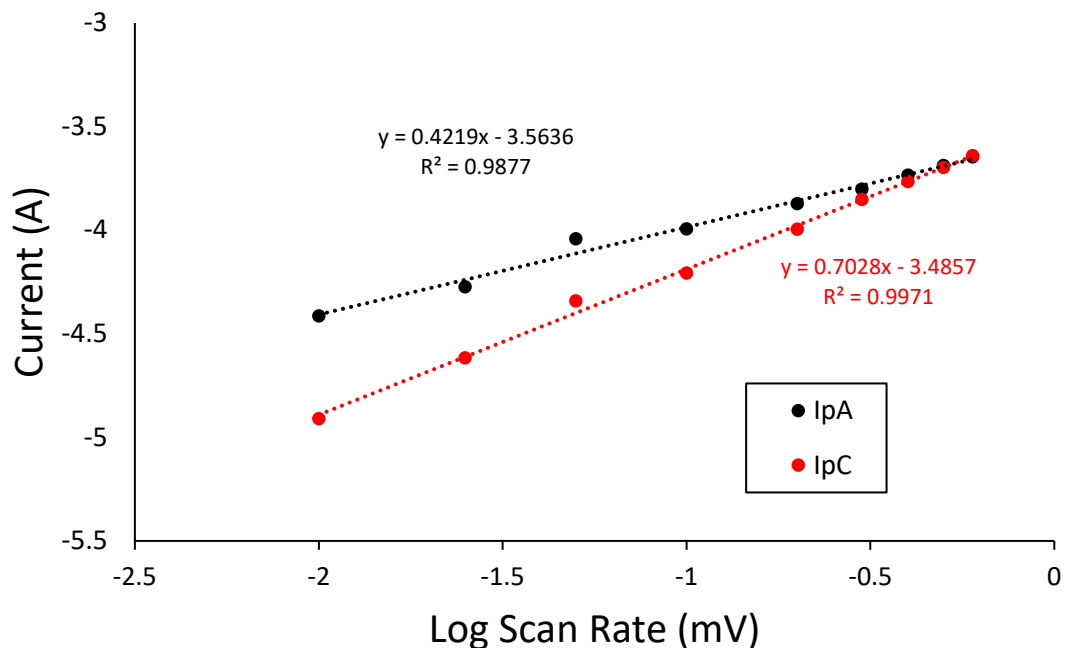
**Figure S3.** Overlay of cyclic voltammograms of various systems from Fig. S2 in 1 mM XYL (150 mM PBS) including **(a)** GCE/PU; **(b)** GCE/ $\beta$ -CD/PU; **(c)** GCE/COOH-MWCNT/PU and; **(d)** GCE/COOH-MWCNT +  $\beta$ -CD/PU (full, optimized modified electrode system). Note: scan rate is 50 mV/sec.



**Figure S4.** DPV oxidative scans of a fully modified electrode (GCE/COOH-MWCNT +  $\beta$ -CD/PU) in PBS (0 mM XYL), 1 mM XYL, and 5 mM XYL showing that the oxidation peak at  $\sim +0.9$  V is sensitive to concentration while the oxidation peak  $\sim +0.0$  V is present without XYL present and is not sensitive to changes in XYL concentration.



**Figure S5-A. (A)** scan rate CVs (Fig. 3) identifying **peaks a and b** analyzed for scan rate dependence (a = XYL oxidation; b = reduction of XYL oxidation product; c = MWCNT oxidation); Example plots for **(B)**  $E_p$  vs Log  $v$ ; **(C)**  $I_p$  vs  $v$  (adsorbed) and; **(D)**  $I_p$  vs  $\sqrt{v}$  (diffusional).

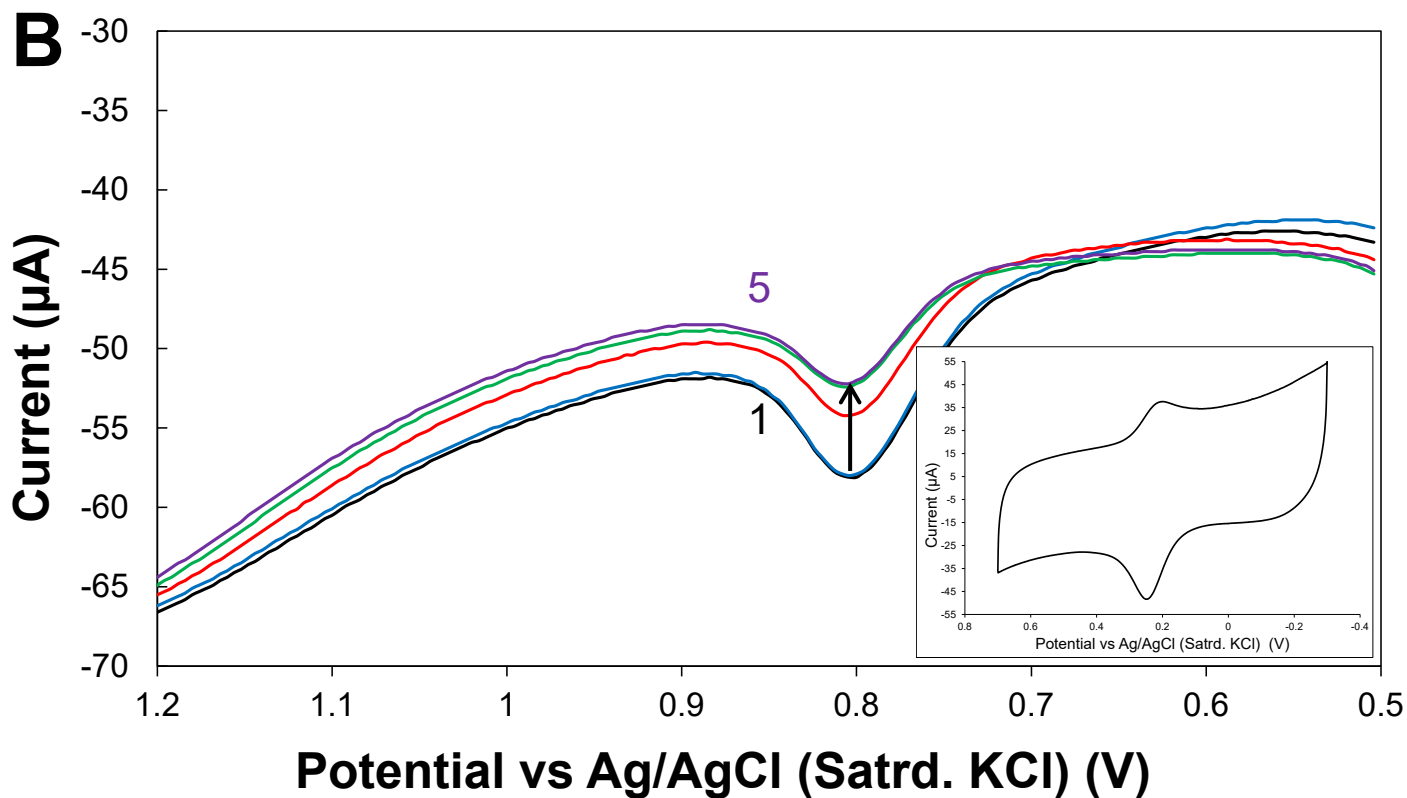
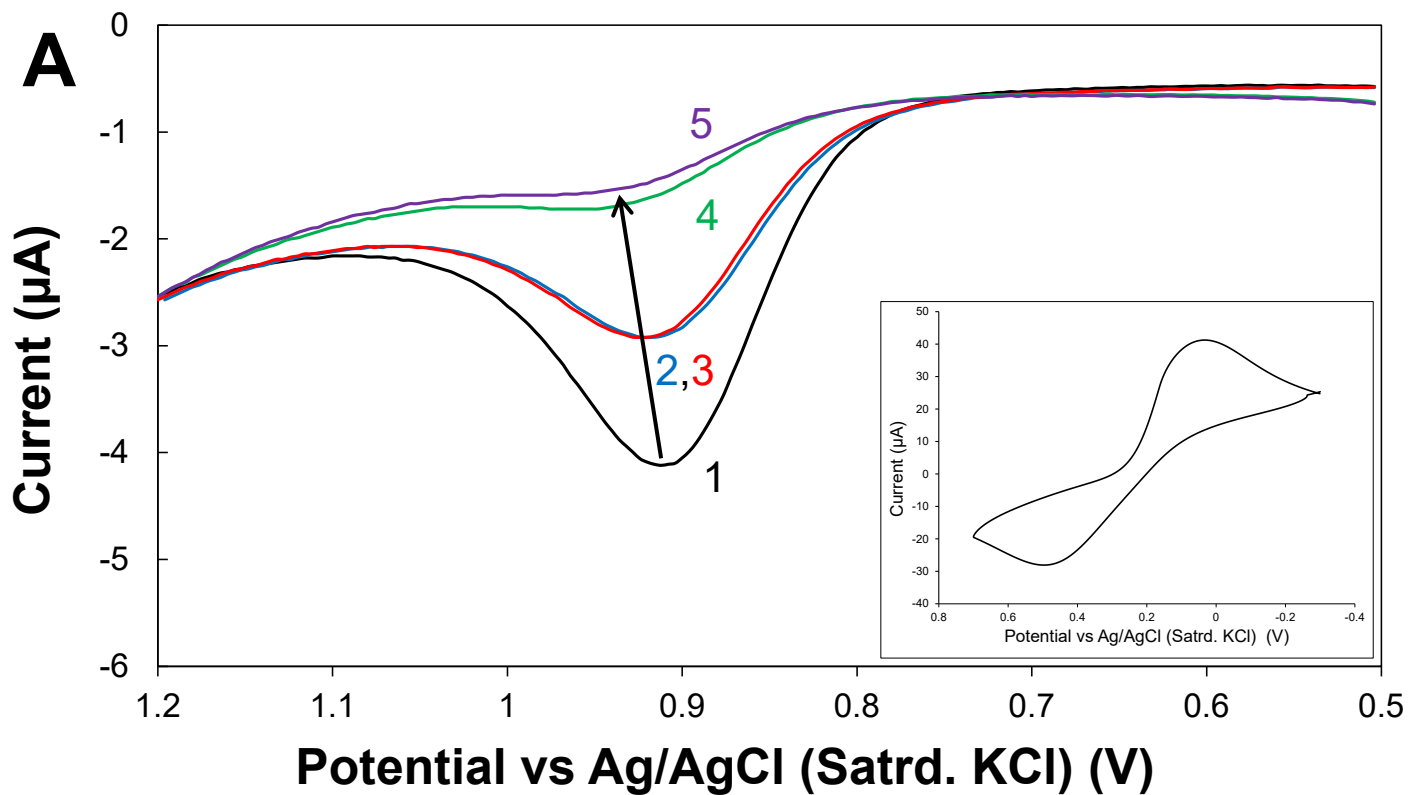
**A****B**

**Figure S5-B. (A)** scan rate CVs (Fig. 3) identifying **peaks a and b** analyzed for scan rate dependence (a = XYL oxidation; b = reduction of XYL oxidation product; c = MWCNT oxidation); **(B)** Example  $\log(v)$ - $\log(i_p)$  plot. Note: Peak c (at  $\sim +0.3$  originally) was analyzed in the same manner with results summarized in Table S1.

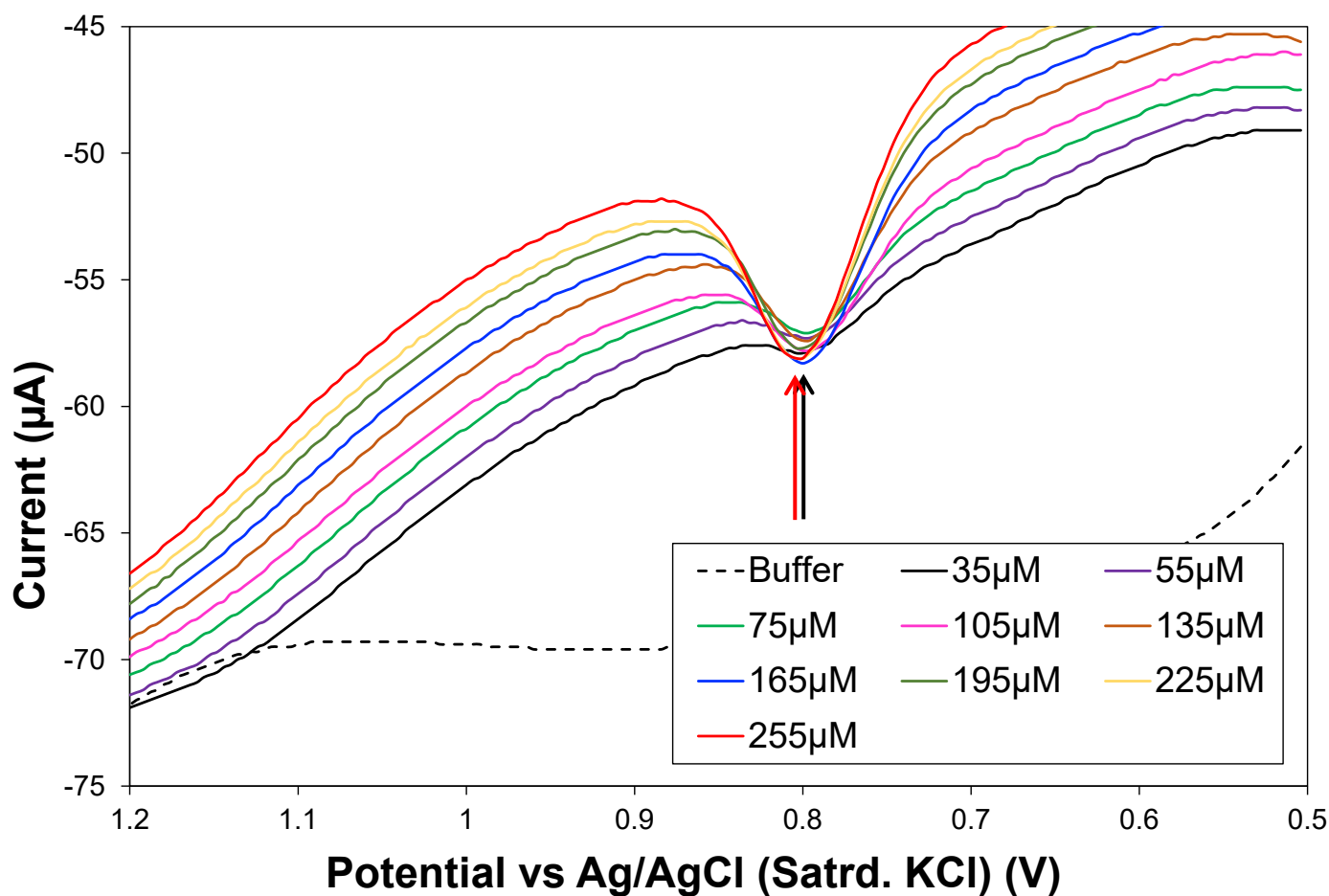


**Table S1: Avg. values for CV scan rate ( $\nu$ ) dependence of 2.5 mM XYL/PBS**

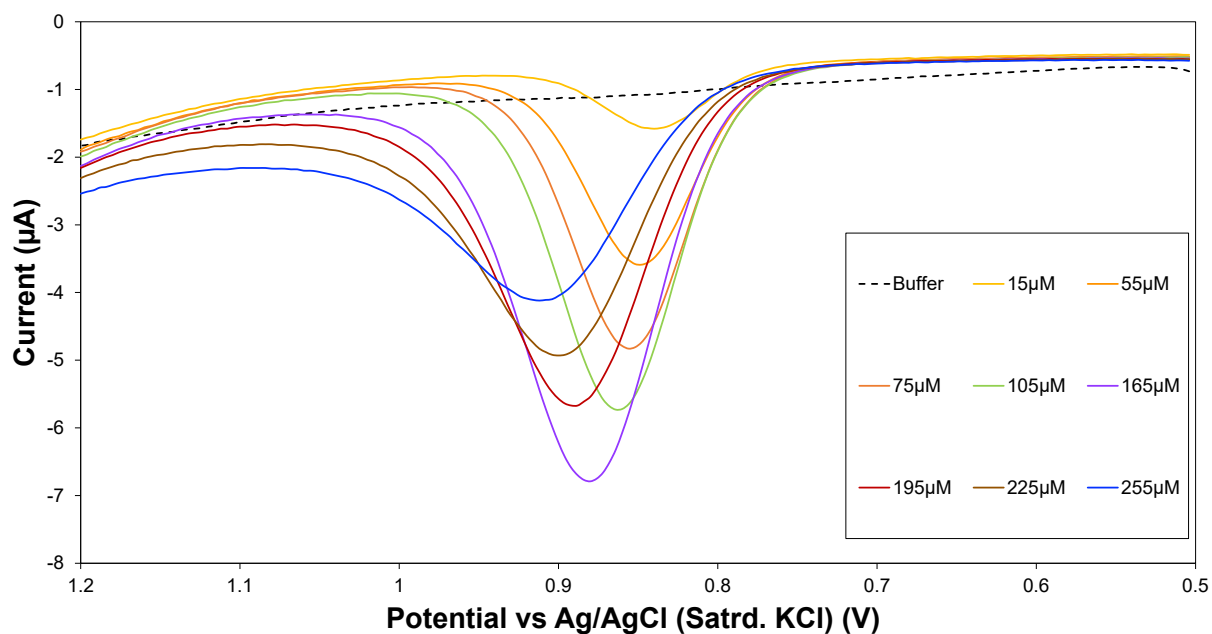
Parameter	(a) Anodic peak at ~ +0.95 V	(b) Cathodic peak at ~ +0.2 V	(c) Anodic peak at ~ +0.3 V
$i_p$ vs. $\nu$ ( $R^2$ )	0.9220 ( $\pm 0.0307$ )	0.9911 ( $\pm 0.0014$ )	0.9806 ( $\pm 0.0090$ )
$i_p$ vs. $\sqrt{\nu}$ ( $R^2$ )	0.9815 ( $\pm 0.0136$ )	0.9882 ( $\pm 0.0011$ )	0.9912 ( $\pm 0.0005$ )
$\log i_p$ vs. $\log \nu$ (slope)	0.4210 ( $\pm 0.0156$ )	0.7094 ( $\pm 0.0316$ )	0.8007 ( $\pm 0.0303$ )
$\log i_p$ vs. $\log \nu$ ( $R^2$ )	0.9794 ( $\pm 0.0128$ )	0.9916 ( $\pm 0.0033$ )	0.9978 ( $\pm 0.0013$ )
Suggested Behavior (adsorbed vs. diffusional)	Diffusional	Adsorbed and Diffusional (mixed)	Adsorbed and Diffusional (mixed)



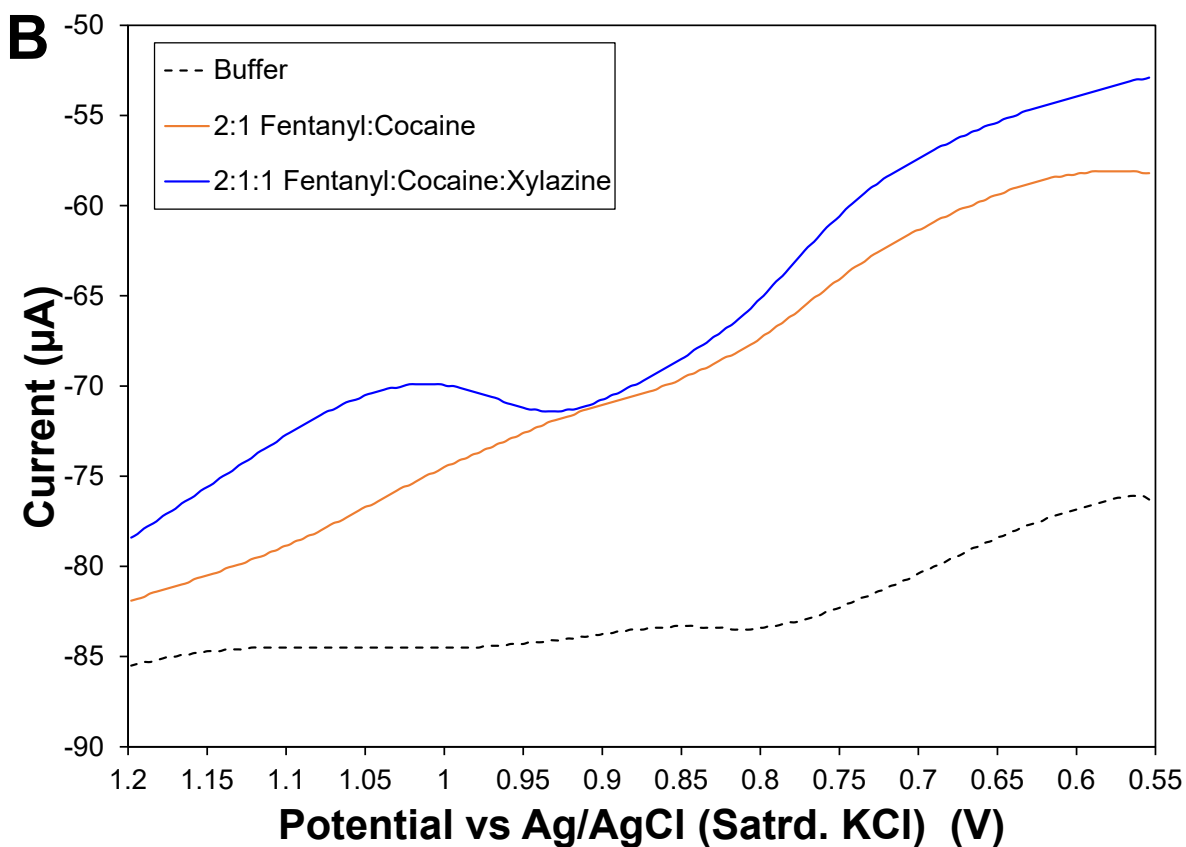
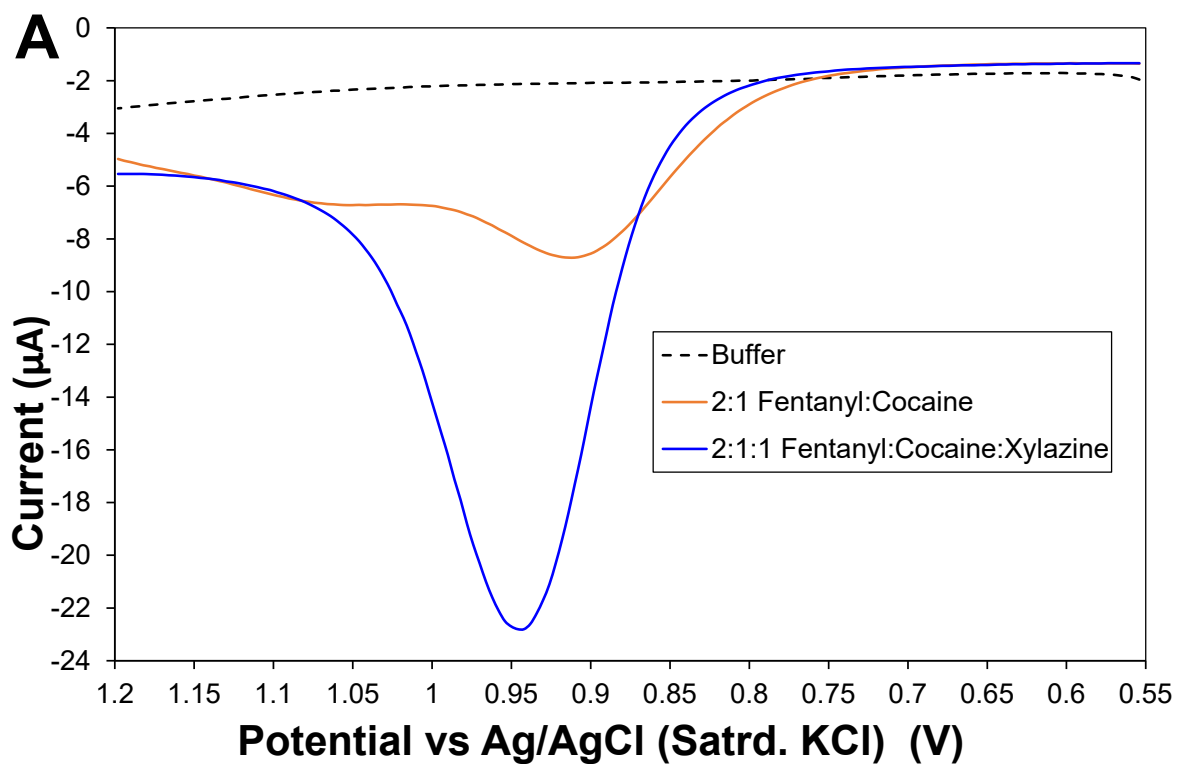
**Figure S6.** Consecutive DPV scans (5) in 255  $\mu\text{M}$  XYL in PBS (150 mM; pH = 7) at a (A) bare and (B) modified GCE showing relative decreases in peak current and peak potential shifts with successive scans; the relative fouling effects are captured by CV of 5 mM potassium ferricyanide (100 mV/sec) after the 5 DPV oxidative scans (insets). Note: Peak definition and an order of magnitude higher current is maintained at the DPV for the modified electrode with essentially no peak potential shift.



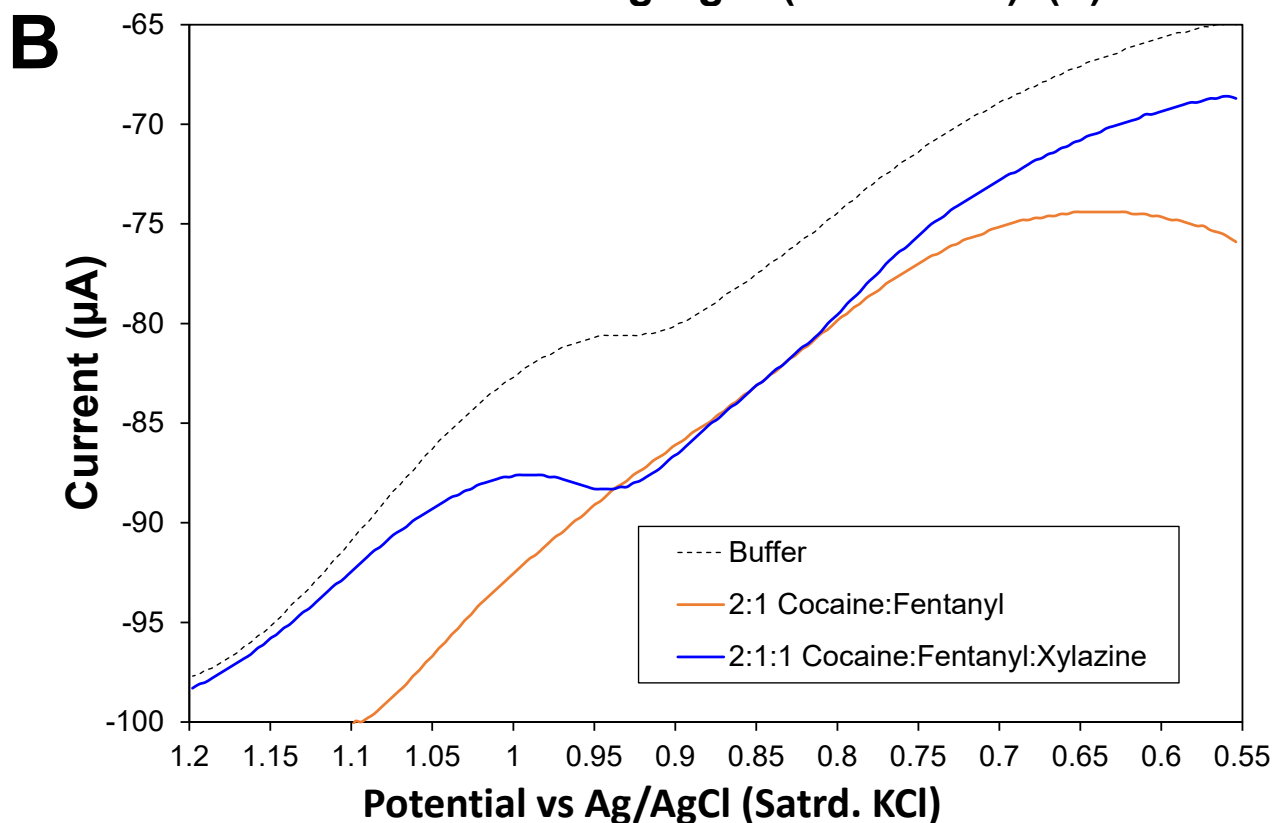
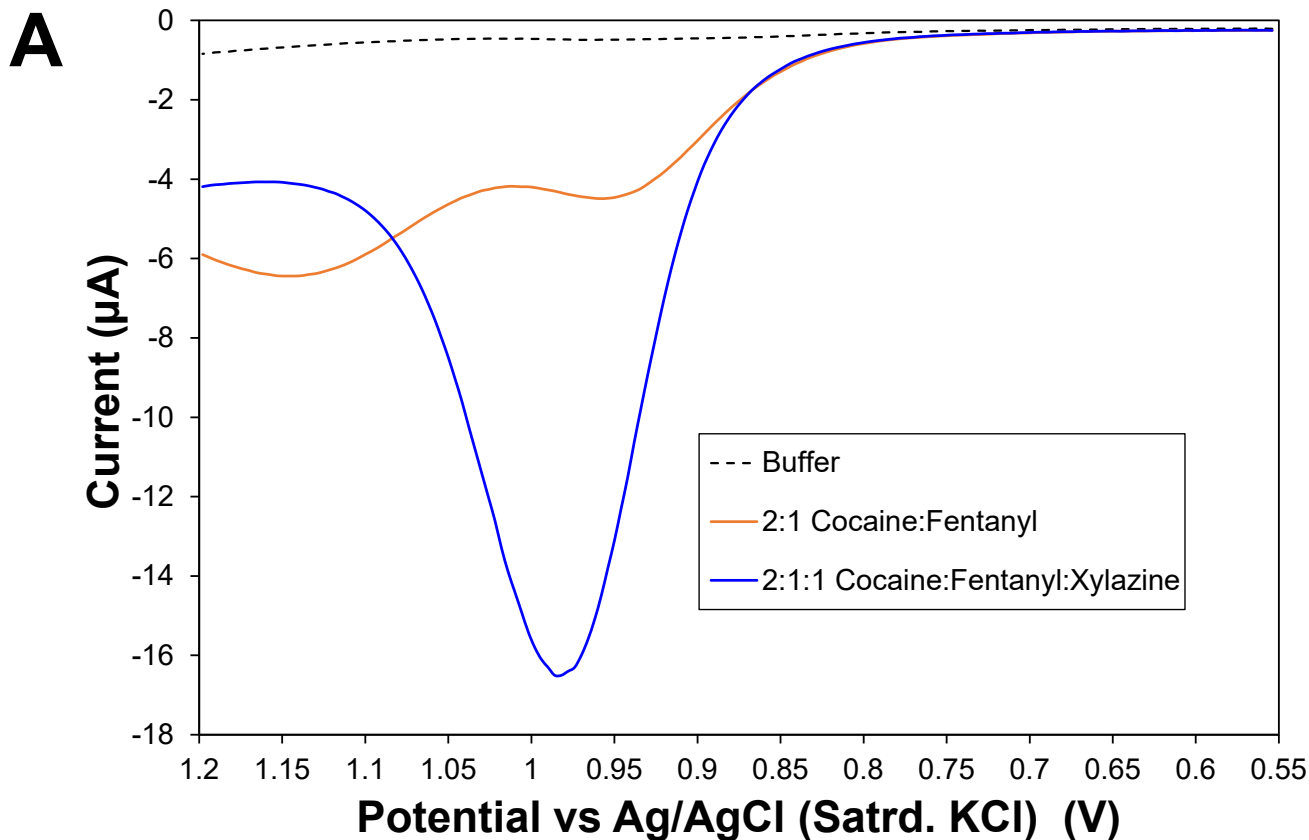
**Figure S7.** All (DPV oxidation scans (all) of a modified GCE exposed to increasing concentrations of XYL to create a standard calibration curve. Note: Only a slight shift in the  $E_{p,a}$  is observed (black and red arrows).



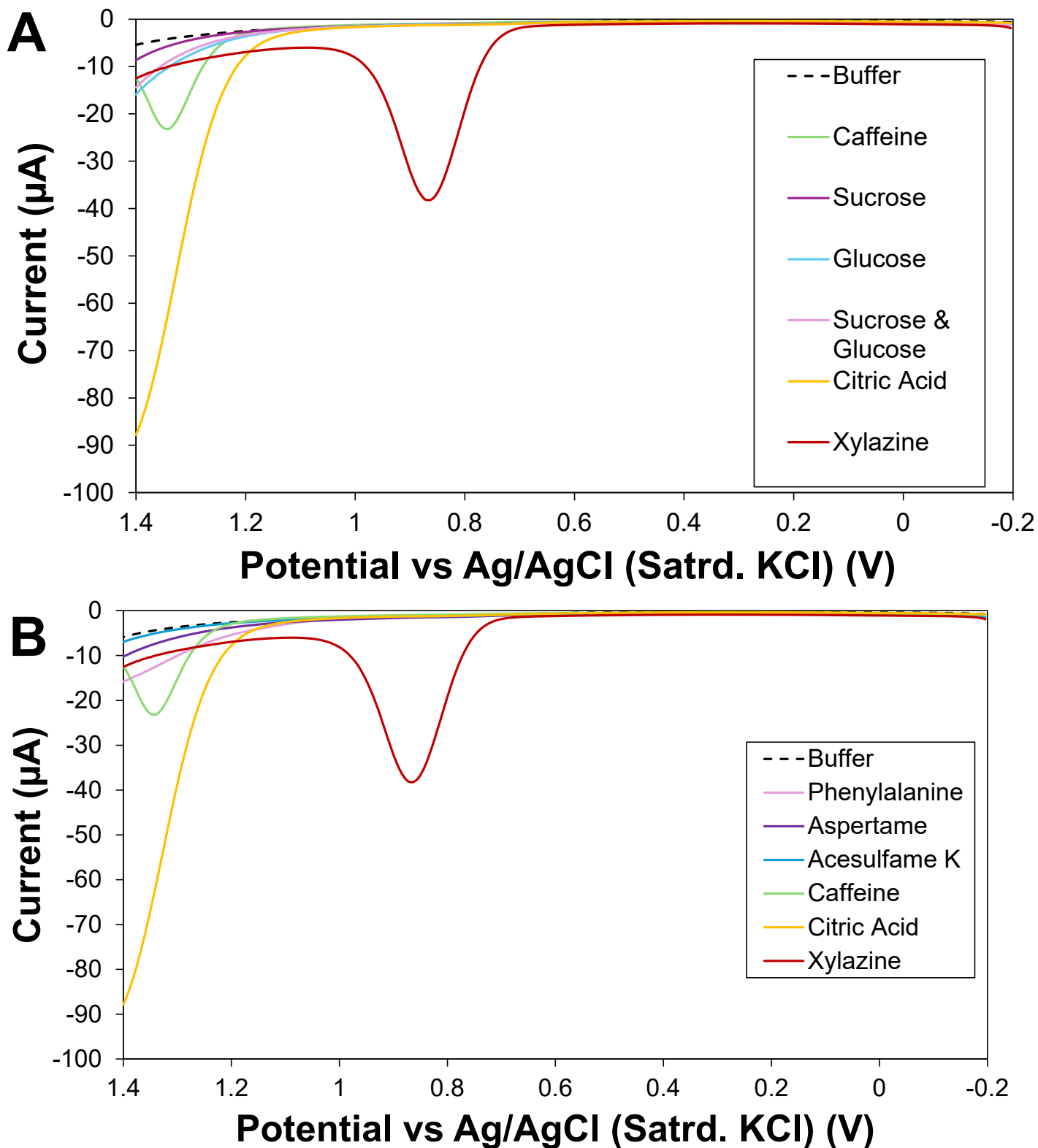
**Figure S8.** DPV oxidation scans (all) of a bare GCE exposed to increasing concentrations of standard XYL. Note: As standard XYL increases, there is a nearly immediate and consistent shift in peak potential while at a certain concentration (165  $\mu\text{M}$ ), the linear relationship between concentration and signal ceases as peak current decreases and peak shape broaden from fouling.



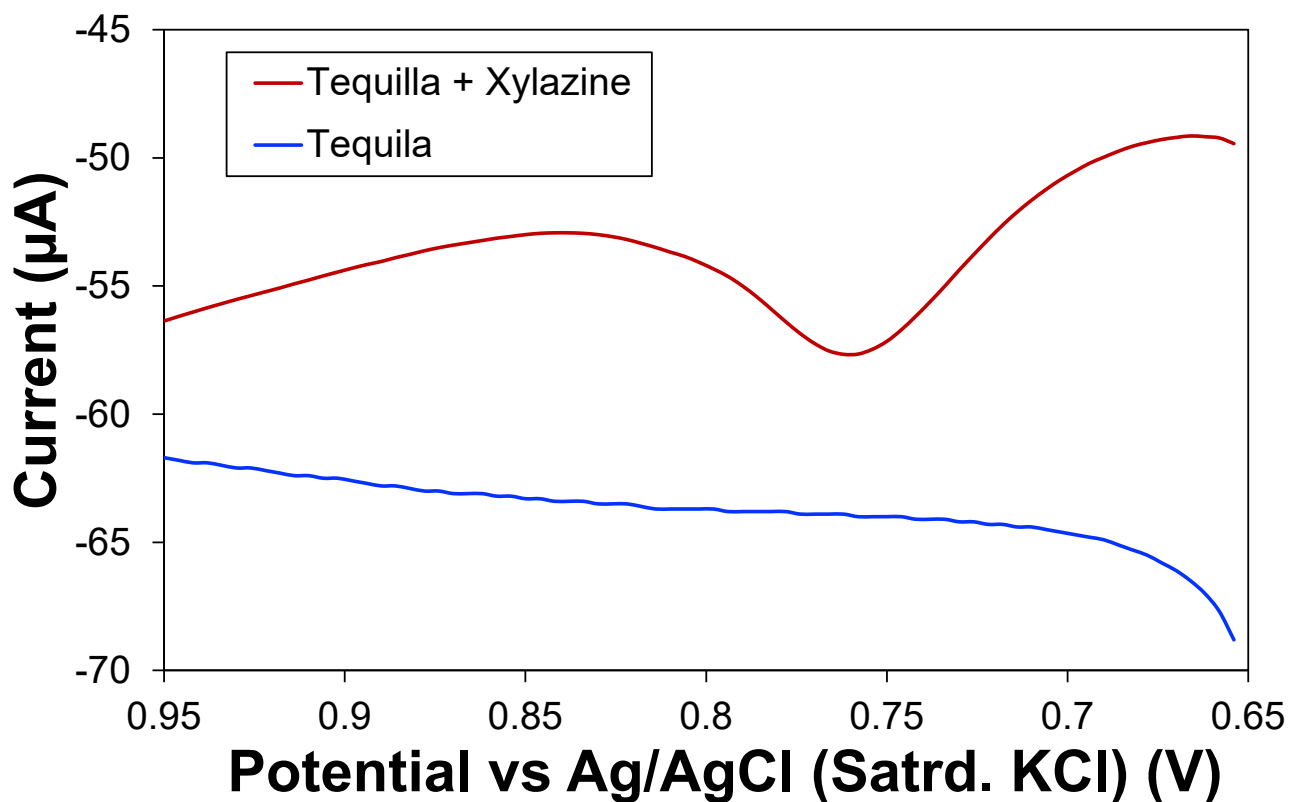
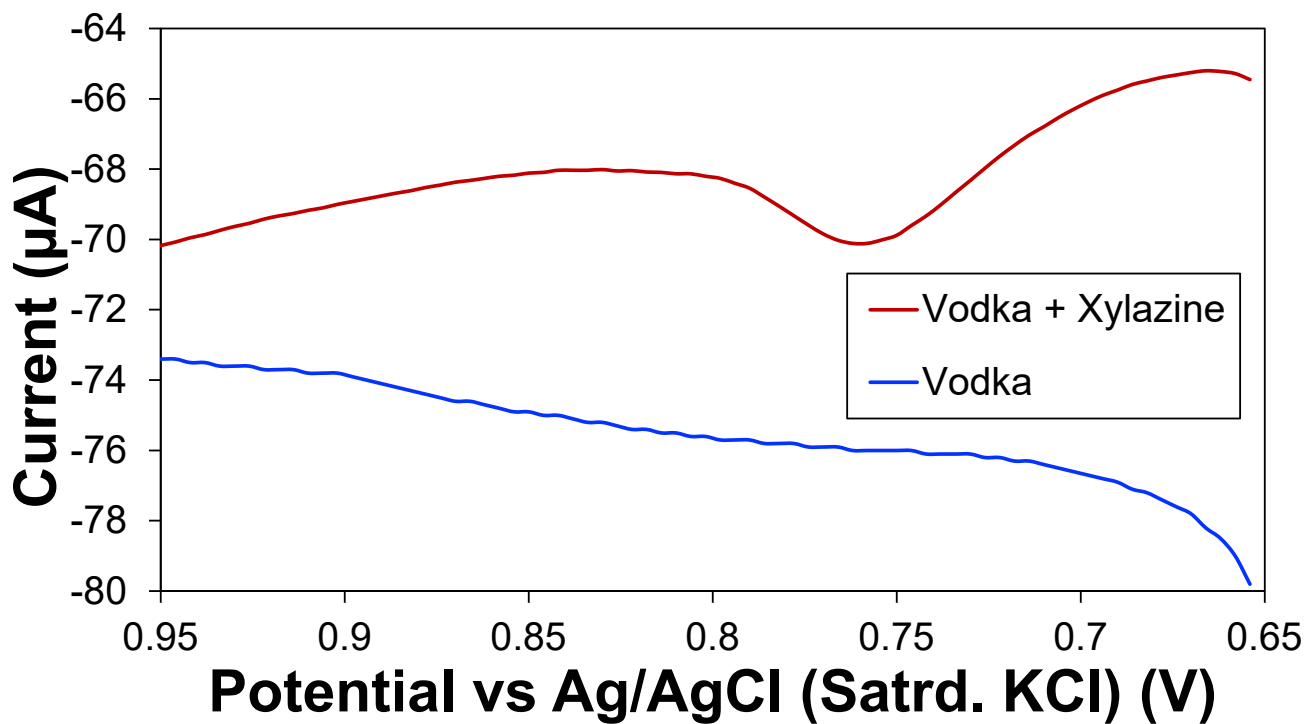
**Figure S9.** DPV scans of **(A)** bare GCE and **(B)** modified GCE in **(a)** 150 mM buffer, **(b)** a mixture of 2:1 fentanyl and cocaine (300  $\mu\text{M}$  : 165  $\mu\text{M}$  ), and **(c)** a mixture of 2:1:1 fentanyl to cocaine to xylazine (300  $\mu\text{M}$  : 165  $\mu\text{M}$  : 165  $\mu\text{M}$  ).



**Figure S10.** DPV scans of (A) bare GCE and (B) modified GCE in (a) 150 mM buffer, (b) a mixture of 2:1 cocaine and fentanyl (330  $\mu\text{M}$  : 150  $\mu\text{M}$  ) and (c) a mixture of 2:1:1 cocaine to fentanyl to xylazine (330  $\mu\text{M}$  : 150  $\mu\text{M}$  : 150  $\mu\text{M}$ ).

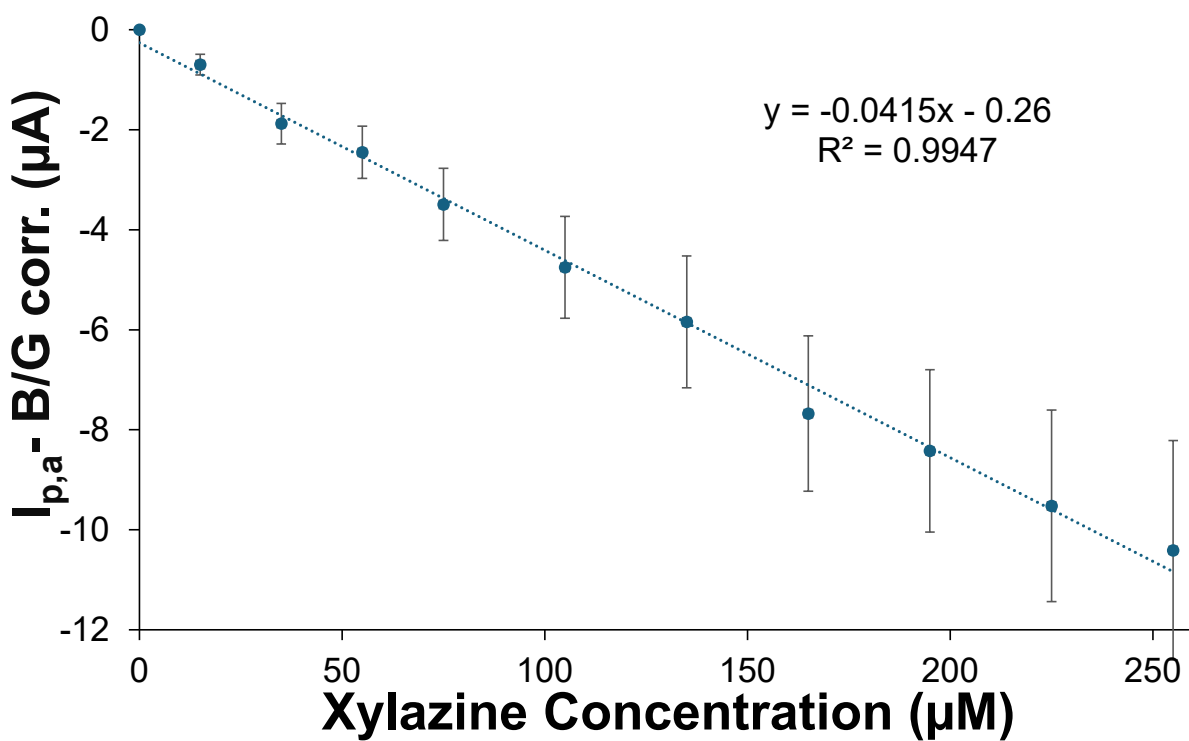
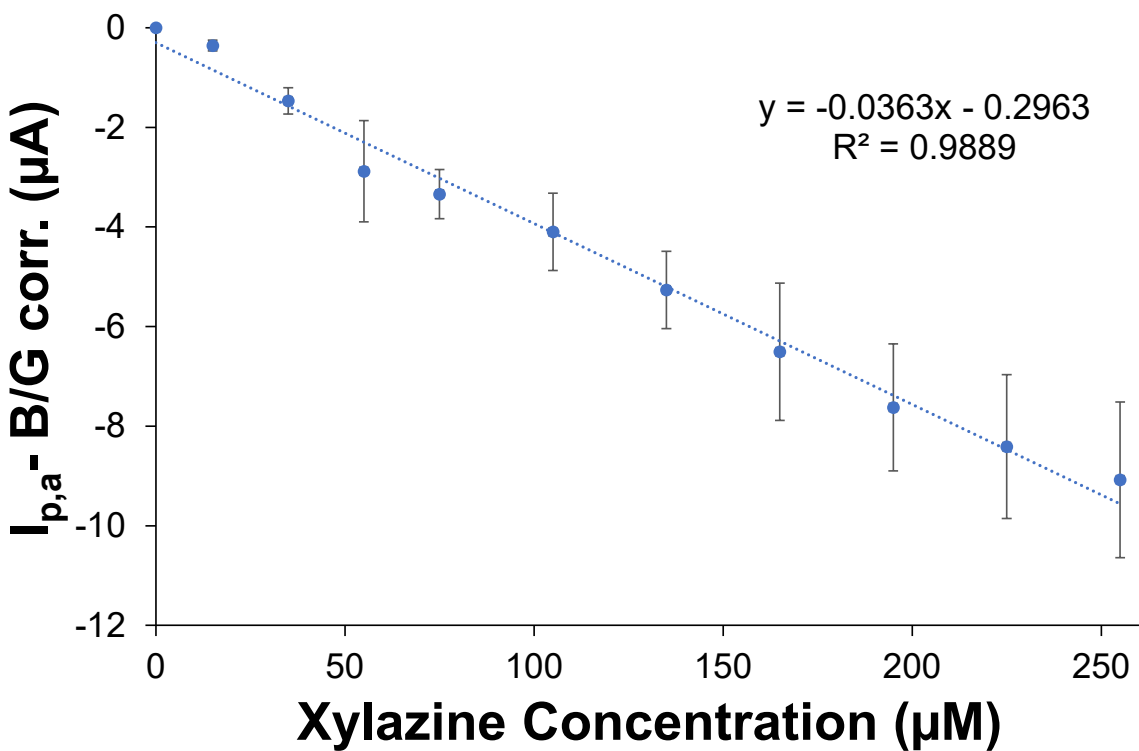


**Figure S11.** DPV oxidation scans of XYL (1 mM) and typical approximate concentrations of common components/interferents in **(A) regular soda:** caffeine (0.50 mM), sucrose (165 mM), glucose (313 mM), mixture of sucrose/glucose (165 and 313 mM), and citric acid (10 mM) and; **(B) diet soda:** caffeine (0.50 mM), citric acid (10 mM); phenylalanine (1.7 mM), aspartame (2.4 mM), and Acesulfame K (0.21 mM) at the modified electrode system.

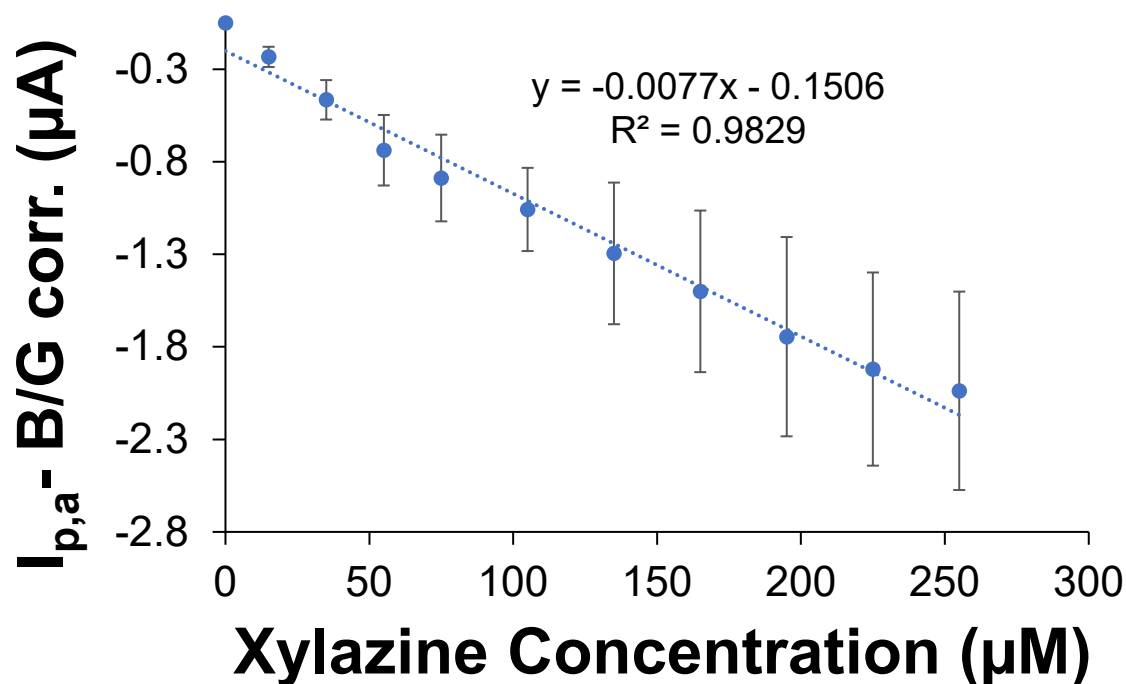
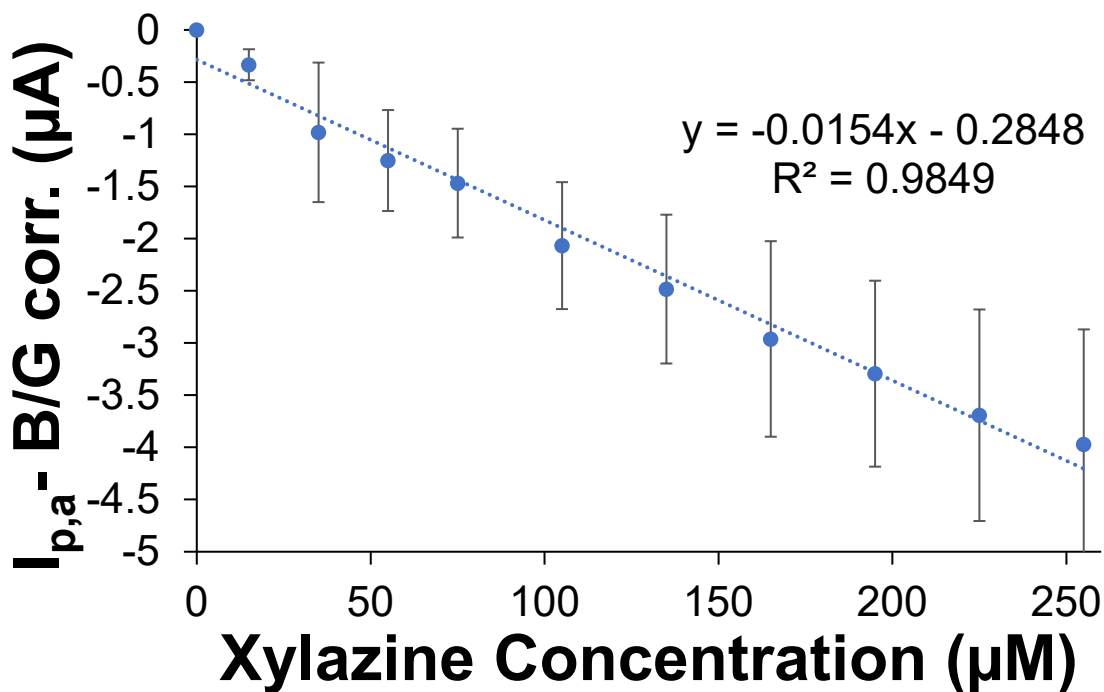


**Figure S12.** DPV oxidation scans of with and without XYL (125  $\mu\text{M}$ ) at the modified electrode system immersed in diluted (A) vodka and (B) tequila samples (1:1 with 150 mM PBS) with results suggesting no interferent-related voltammetric peaks from the beverage matrices in either case.

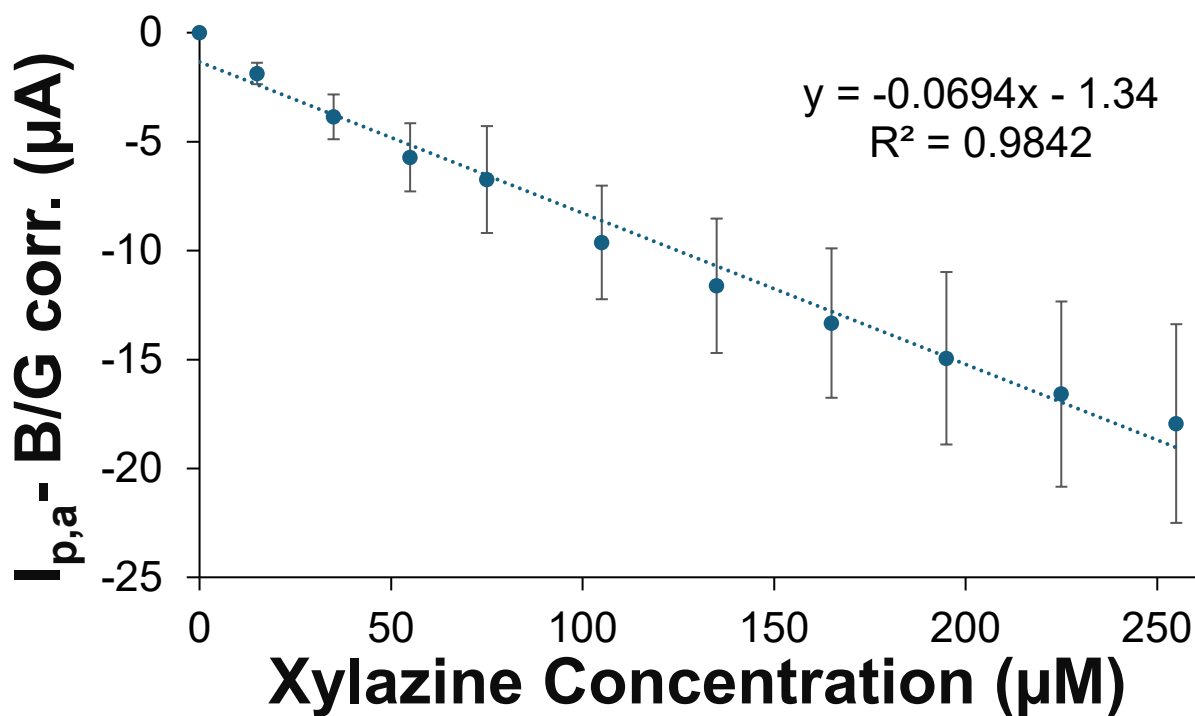


**A****B**

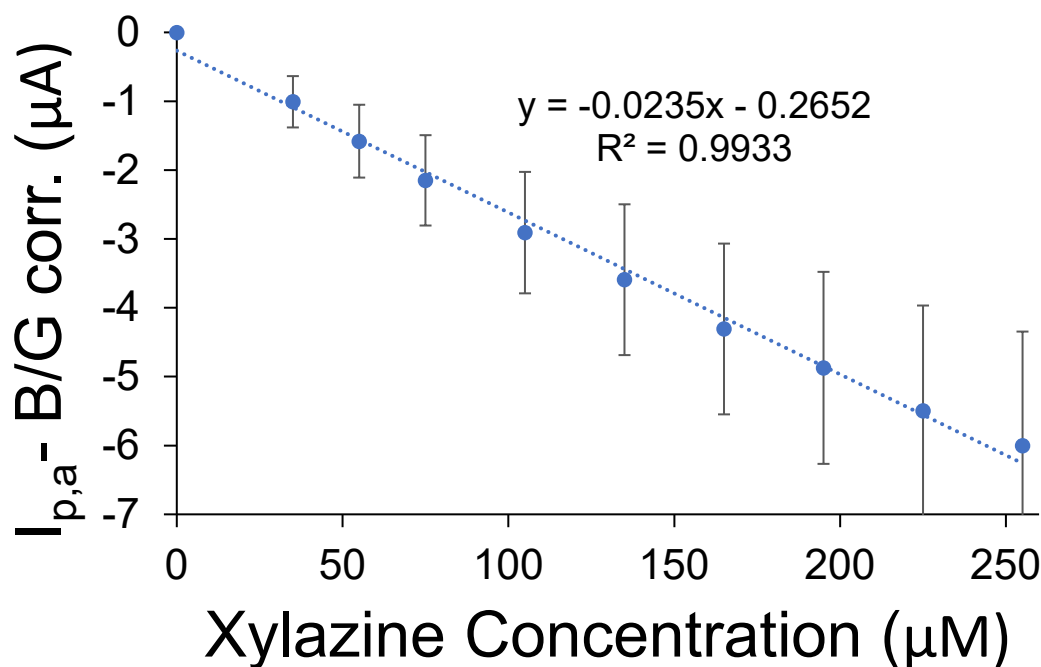
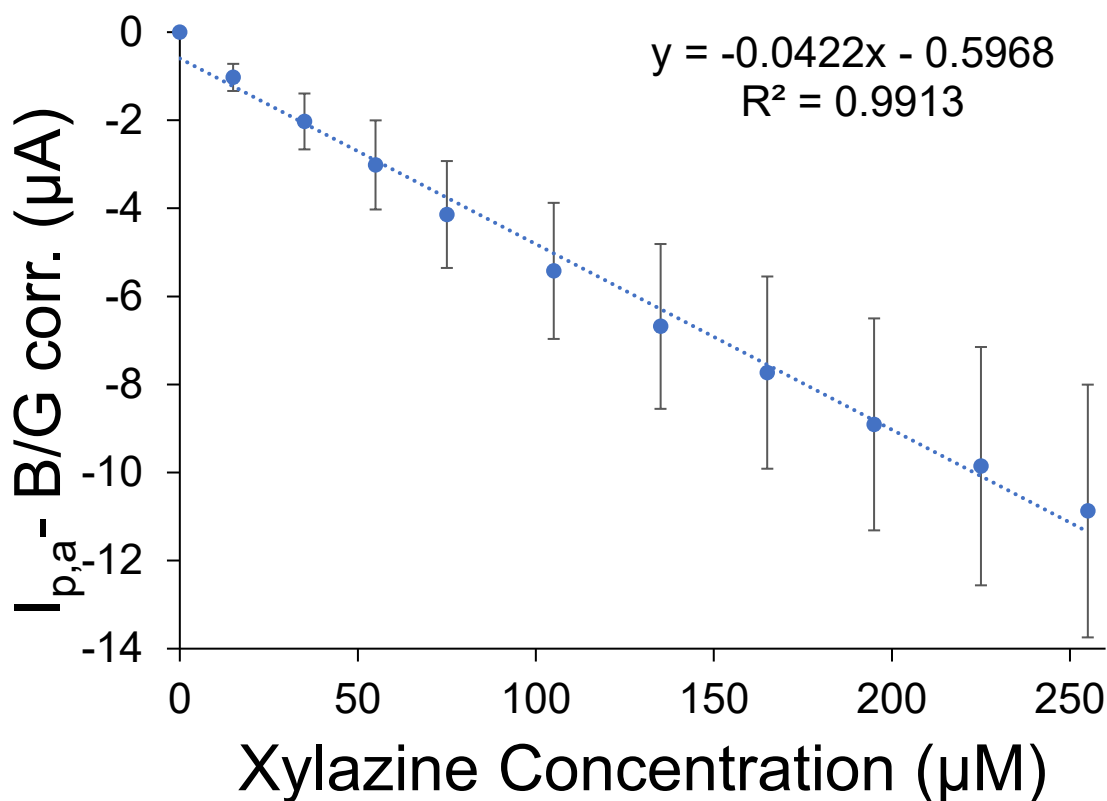
**Figure S13.** DPV generated XYL standard calibration curves for **(A)** simulated soda solution and **(B)** simulated diet soda solution.

**A****B**

**Figure S14.** DPV generated XYL standard calibration curves for (A) cola and (B) diet cola solution (undiluted).



**Figure S15.** DPV generated XYL standard calibration curves for diluted (1:1, 150 mM PBS) cola.

**A****B**

**Figure S16.** DPV generated XYL standard calibration curves for (A) tequila and (B) vodka solutions. NOTE: Beverages were diluted with 150 mM PBS in a 1:1 ratio .